Kick-scooters detection in sensor-based transportation mode classification methods

Fadoua Taia Alaoui, Hassen Fourati, Alain Kibangou, Bogdan Robu, Nicolas Vuillerme

Kick-scooters detection in sensor-based transportation mode classification methods ⋆

F. Taia Alaoui * **H. Fourati** * **A. Kibangou** * **B. Robu** * **N. Vuillerme** **

* *Univ. Grenoble Alpes, CNRS, Inria, Grenoble INP, GIPSA-lab, F-38000 Grenoble (e-mail: hassen.fourati@gipsa-lab.fr)(corresponding author)*
** *AGEIS, University Grenoble Alpes, Grenoble, France*

Abstract: In this work we present a novel classification model that can detect kick-scooters from inertial and pressure sensors. The detection is performed with kick-scooters being trained with other activities and transportation modes including still, walking, biking, taking bus and tramway. Results show that kick-scooters can be precisely detected up to 99% for three different sensor placements: on-foot, waist-attached and in the trouser's pocket. Thus, this paper provides a first contribution where kick-scooters can be classified and studied for further applications such as mobility behavior analysis and navigation.

Keywords: Transportation mode detection, kick-scooters, urban transport, convolutional neural networks, deep learning.

1. INTRODUCTION

Micro-mobility refers to lightweight and speed-limited urban locomotion. Recently, it has become part of the global urban transportation ecosystems. Within the large range of existing micro-vehicles, such as bikes, segways, mono-wheels, skateboards, or hoverboards, kick-scooters together with bikes seem to be the most popular even among adults and seniors. For instance, the Priestman-Good's kick-scooter for life [1] was specifically designed to promote physical activity for the elderly. Furthermore, kick-scooters seem to be an effective solution to the problem of the first mile last mile (FMLM) distance, McKenzie (2020), i.e. the distance between home or work and the nearest public transport station. In fact, transit accessibility was found to be highly increased by the use of bikes over walking to travel the FMLM distance, Zuo et al. (2020). Though, the same conclusion could be made for any other micro-vehicle since the important factor is the speed of motion. Note that the lack of speedy mobility is an increasing factor to travelling the FMLM distance by individual motorized vehicles, Shiv et al. (2018). The popularity of kick-scooters can further be explained by their efficiency in meeting both the citizens need for rapidity and availability, as they can be parked easily due to their small size; they can also be folded for a major part of them, and therefore can be carried in public transport, unlike bicycles, but they additionally meet the environmental requirements of a green and smooth mobility as they are either human powered or electric. From the infrastructure usage perspective, kick-scooters are pretty convenient as they are allowed to share bike lanes and other public spaces, Kostrzewska and Macikowski (2017). In summary, kick-scooters seem to be user-friendly, healthy, and recreational for both adults and younger populations, Kostrzewska and Macikowski (2017). Yet, they are still not much considered in recent researches dedicated to transportation mode detection (TMD) methods, whereas travel mode information is crucial for analyzing mobility behaviors and adapting policies to environmental and traffic challenges. This paper aims at filling this gap through the elaboration of a classification model that recognizes kick-scooters among other transportation modes that include on-foot activities, bike, tramway, and bus.

The integration of kick-scooter detection is novel to TMD methods. To the best of the authors knowledge, the only study that has ever considered classifying kick-scooter data, Prentow et al. (2015), was based on a dataset containing only 10 minutes of kick-scooter signals from an unknwon number of participants. Thus, as a first step towards the integration of kick-scooters to the global landscape of common TMD methods, we use an improved database of 48 hours collected by 34 participants, including 4 hours of kick-scooter signals from 18 participants using low-cost inertial and pressure sensors. With this dataset, we suggest two classification models selected based on the accuracy of kick-scooter detection for 3 different placements of the sensors: on-foot, waist-attached, and in the trouser's pocket.

⋆ This work was part of the project CAPTIMOVE funded by the IDEX of University Grenoble Alpes (call for projects "Initiatives de Recherche Stratégiques (IRS)") (ANR-15-IDEX-02). This work was also supported by the French National Research Agency in the framework of the Investissements d'avenir program (ANR-10-AIRT-05). The sponsors had no involvement in the design of the study, the collection, analysis and interpretation of data, and in writing the manuscript. This work further forms part of a broader translational and interdisciplinary research program, GaitAlps.The graphical content used in this paper was designed by macrovector / Freepik and Flaticon.com.

[1] `https://www.priestmangoode.com/project/scooter-for-life/`

The paper is organized as follows: Section 2 presents an overview of existing TMD studies. Section 3 presents data collection. Section 4 is about the classification approach. Section 5 provides the results of the classification. Section 6 is a brief conclusion of this work.

2. RELATED WORKS

Several technologies have been used for TMD purposes. For example, Global Positioning Systems (GPS), Xiao et al. (2015), or mobile networks, Huang et al. (2019). Besides, Geographical Information Systems (GIS), Gong et al. (2012), Semanjski et al. (2017), have been a valuable aid to these methods. Less common are methods based on Bluetooth or Wireless Fidelity (WIFI), Coroamă et al. (2019). Also, inertial sensors have been extensively used for TMD purposes: accelerometers, Liang and Wang (2017), gyroscopes, Zhao et al. (2019), barometers and magnetometers, Su et al. (2017). More recently, microphones have also shown promising TMD results, Carpineti et al. (2018). In general, multiple data sources are fused to increase the classification accuracy. For example, accelerometer and GPS, Shafique and Hato (2015), inertial sensors and a microphone in Carpineti et al. (2018), inertial sensors, a light sensor, a barometer, and a magnetometer in Su et al. (2017).

As for the considered transportation modes, a refining of TMD classifications has been observed through time. While only on-foot versus few vehicle modes were recognized in the first TMD works, Gonzalez et al. (2010), today car, Gonzalez et al. (2010), bus, Shafique and Hato (2015), train, and metro, Wang et al. (2019), have all been considered individually. Furthermore, electric bikes (E-bike) versus human-powered bikes were distinguished in Xiao et al. (2015). Recently, combined indoor-outdoor TMD works have also been developed, Taia Alaoui et al. (2021). Kick-scooters have been considered in Prentow et al. (2015) with a very limited sample size of 10 minutes.

Previous TMD studies have shown that decision trees and more specifically random forests (RF) are the most efficient in the case of TMD problems, Carpineti et al. (2018), Lorintiu and Vassilev (2016), Wang et al. (2018). Lately, many studies suggested that neural networks also provide satisfying results, for example feed-forward neural networks (ANN), Fang et al. (2017), convolutional neural networks (CNN), Liang and Wang (2017), and long-short term memory (LSTM) neural networks, Asci and Guvensan (2019). Generally, several algorithms are compared for model selection, Carpineti et al. (2018), Wang et al. (2019).

In terms of dataset, few databases are publicly available, Carpineti et al. (2018), Yu et al. (2014). Overall, the sample size, i.e. number of participants, is generally low or absent. For example, this information is lacking in Liang et al. (2019), Liang and Wang (2017), Asci and Guvensan (2019) and Ballı and Sağbaş (2017). On the other hand, few studies indicate the placement of the sensors on the body, Zhao et al. (2019), Wang et al. (2019), and Ahmed et al. (2019). Thus, these discrepancies in terms of sample size and data description and availability, together with the differences in adopted classifications, make the major part of TMD studies unreproducible. One of the objectives of this study is to allow reproducibility and provide enough information on the database construction and the methodological approach.

3. DATA COLLECTION

In this study, 34 healthy adults volunteered for the experiments, 20 males and 14 females. They were aged from 18 to 50. Experiments were led during workdays at different hours, including rush hours (8-9am, 12-2pm, 4-6pm) and under different weather conditions (sunny, cloudy, rainy). The trips were planned in advance using an experimental protocol document given to the participants together with a data use agreement at the moment of their arrival. They were equipped in the laboratory office and were accompanied during the whole experiment by the person in charge of later labelling the data. In the experimental protocol, 2 different buses and tramways had to be taken by each participant in order to vary the signal patterns relative to each vehicle. For biking and scooter-riding, a minimum trip duration was imposed. However, participants were free to make longer trips for these two transportation modes. 18 subjects collected data from a kick-scooter. They were asked to switch legs during experiments in order to prevent any biases related to the choice of the pushing leg. The total number of used kick-scooters was 6. The left locomotion modes involved at least 20 different participants and included walking, biking, and taking public transport (tramway, bus). However, some of these classes have more than 20 participants, such as walking with a number of 34 participants. The recordings were made using 3 Inertial Measurements Units (IMUs) that include a 3-axis accelerometer, a 3-axis gyroscope and a barometer each. They were placed on the foot, on the waist and in the trousers' pocket (Fig. 1). The smartwatch, camera, wrist-worn, and hand-held IMUs are of not interest in this study. The total time duration of the data collected is around 48 hours. The total duration of collected signals for each locomotion mode is given in Fig. 2. This dataset was publicly released and can be accessed through this link [2]. The data used in this work were subsampled at a frequency of 32Hz.

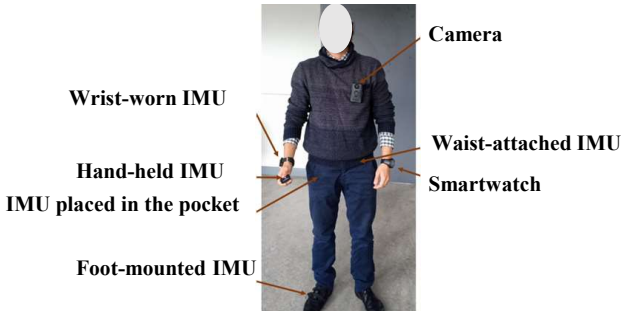

Fig. 1. Placement of the sensors on the body

4. CLASSIFICATION APPROACH

4.1 Adopted classification

Fig. 3 shows the adopted classification in this paper that consists of 5 classes: Still - Walk - Bike - Public Transport

[2] https://perscido.univ-grenoble-alpes.fr/datasets/DS310

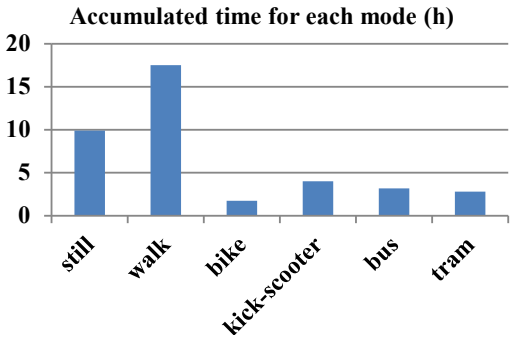

Fig. 2. Accumulated time duration for each transportation mode

(PT), resulting from the fusion of tramway and bus, and Kick-scooter (KS).

Fig. 3. Transportation modes considered in this study

4.2 Pre-processing of signals

In order to remove peaks that are isolated and that do not relate to the transportation modes (eg. somebody touching their head or moving hands), signals have been pre-processed as follows:

- Acceleration and angular rate: a sliding window of 1sec was used to computed signal frames, without overlapping. Based on the boxplot of each signal frame, the upper and lower outliers were respectively replaced by the maximum and minimum of the boxplot. This processing was applied to each axis independently before computing the signals norms.
- Atmospheric pressure: Due to high frequency noise in measured pressure, the raw signal was replaced by its average envelope.

In addition, all signals were standardized according to equation (1) in order to avoid any training biases related to scale and unit.

$$Scaled(X_k) = \frac{X_k - \mu}{\sigma} \tag{1}$$

where X_k is the k^{th} term of the time series X to be scaled, μ is the mean of the time series and σ is its standard deviation.

4.3 Classification algorithms

A CNN and RF have been selected in this work. Their architecture is unique to this classification problem. For RF, the model designing is rather intuitive as it consists in only choosing the number of trees, which is 60, and the number of features to be used in each tree, which is 8. The chosen split criterion is the Gini index. For the CNN, multiple tests have been performed by varying the model architecture (number of layers) and parameters (learning rate, optimizer, etc.) for model selection. The CNN architecture consists of 3 convolutional layers of 30 filters each. The kernel (or filter size) was respectively of 3/8sec for the first layer, 3/4sec for the second, and then 3/2sec for the last convolutional layer. This way, the kernel was first chosen very small and was gradually increased in order to catch different data structures inside signal frames. A Maximum pooling of 2 was chosen after each convolutional layer. Two fully connected dense layers relate the convolutional layers to the neural network output layer. They have respectively 200 and 50 neurons. The chosen activation function for the three convolutional layers was LeakyRelu with an Alpha (or slope) value equal to 0.1. The activation function of the dense layers was the relu function. The output layer which has 5 neurons corresponding to the classes has a softmax activation function. The cost function was the categorical cross-entropy. The chosen optimizer was Adam, with a learning rate initialized at 0.01. The stopping criterion was based on the validation loss.

4.4 Feature computation

Data were manually segmented and labelled by an expert person according to a segmenting window of 3sec that was empirically chosen. Afterwards, time and frequency-domain features were calculated, see Table 1. The features computed in this study can be also found in the literature such as in Wang et al. (2019). RF automatically selects the most relevant features while constructing the different decision trees. For the CNN, we chose to train the algorithm directly using the preprocessed signal frames rather than using descriptive features. In fact, ordering descriptive features as if they were an image, for example in Yanyun et al. (2017), may result in totally different models based on the order of the features. Besides, this order lacks physical equivalent, while the internal structure of a time sequence remains relevant and does not interfere with the model design.

4.5 Statistical tools to assess the classification performance

A 3 fold-cross validation process was realized. Therefore, the confusion matrices given in section 5 have float terms. In each fold, 70% of labelled data were used for training and the left 30% were used for validation. The statistical tools used to evaluate the classification are valid for a binary classification, and for multi-class problems by recursively considering each class as Positive and all others as Negative. Then, each confusion matrix has 4 types of data: True Positives (TP), True Negatives (TN), False Positives (FP), and False Negatives (FN). Due to the unequal time-distribution of the transportation modes, the overall accuracy is provided together with the macro-averaged F1-Score as the latter is not sensitive to class distribution. Details about these accuracy metrics can be found in Hossin and Sulaiman (2015). In this work, confusion matrices have columns dedicated to ground truth, and rows dedicated to predictions.

In terms of data size, 510532 samples were used for training and 170178 for testing with the foot-mounted sensor, 473574 for training and 157858 for testing with the waist-attached sensor, and 491778 train samples and 163927 test samples with the sensor placed in the trouser's pocket.

Table 1. Training dataset composition

Signal channel	Features
Acceleration norm (norm acc), Gradient of the norm of acceleration (grad acc), Integral of the norm of acceleration (int acc), Angular rate norm (norm gyr), Gradient of the norm of angular rate (grad gyr), Integral of the norm of angular rate (int gyr)	Mean, Energy, Standard deviation, Variance, Main frequency component, Power of the main frequency component, Spectral energy between 0 and 2Hz, Spectral energy ratio between 0 and 2Hz, Spectral energy between 2 and 4Hz, Spectral energy ratio between 2 and 4Hz, Spectral energy between 4 and 10Hz, Spectral energy ratio between 4 and 10Hz, Spectral energy between 10 and 30Hz, Spectral energy ratio between 10 and 30Hz, Spectral centroid, Spectral spread, Entropy, Number of zero crossings
Smoothed pressure (pres)	Spectral centroid, Spectral Spread, Number of zero crossings after scaling, Main frequency component, Power of the main frequency component, spectral energy between 0 and 2Hz, Spectral energy ratio between 0 and 2Hz, Spectral energy between 2 and 4Hz, Spectral energy ratio between 2 and 4Hz, Spectral energy between 4 and 10Hz, Spectral energy ratio between 4 and 10Hz, Spectral energy between 10 and 30Hz, Spectral energy ratio between 10 and 30Hz
Gradient of smoothed pressure (grad pres) and integral of smoothed pressure (int pres)	Mean, Min, Max, Standard deviation, Main frequency component, Power of the main frequency component, Spectral centroid, Spectral spread, Number of zero crossings

5. CLASSIFICATION RESULTS AND ANALYSIS

5.1 RF Algorithm

Feature importance Fig. 4, Fig. 5 and Fig. 6 show the computed importance of each input feature. Two thresholds were chosen to create 3 feature importance groups: the highest in red, average in green and the lowest in blue. The features are given numbers from 0 to 139. From these figures, it is observed that the same signal channels do not have the same importance depending on the placement of sensors. For instance, for the foot-mounted sensor, the most important features are based on the gradient of acceleration (feature number between 18 and 36). We observe a strong concentration of the important features in this channel over all the left ones. For the waist-attached sensor, the acceleration norm (between 0 and 17) seems more important than the gradient of acceleration. The gradient of pressure and pressure-based features are also classified as highly important (between 108 and 139). Finally, for the sensor placed in the trouser's pocket, the distribution of the most important features is sparse and involves first the pressure-based features, the gradient of acceleration, the integral of acceleration (37-55), and the gradient of angular rate (75-93).

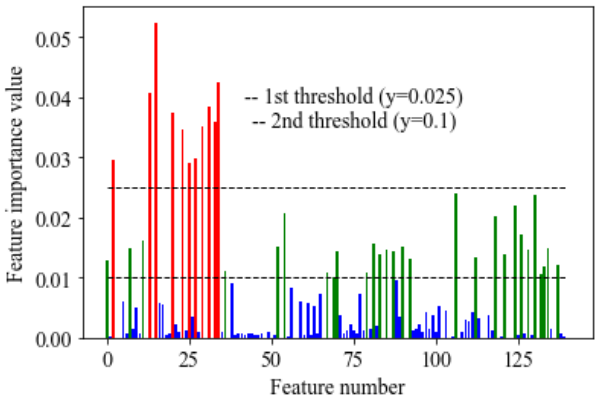

Fig. 4. Feature importance for the foot-mounted sensor

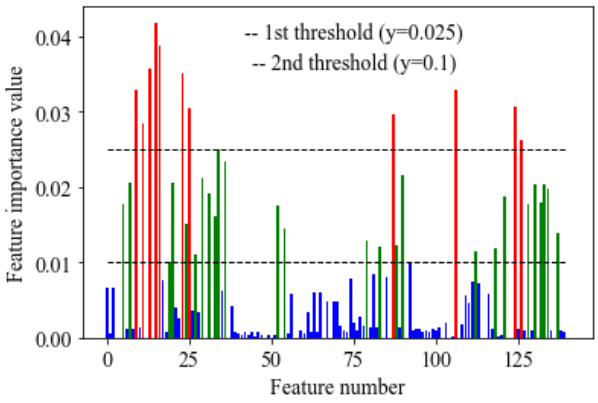

Fig. 5. Feature importance for the waist-attached sensor

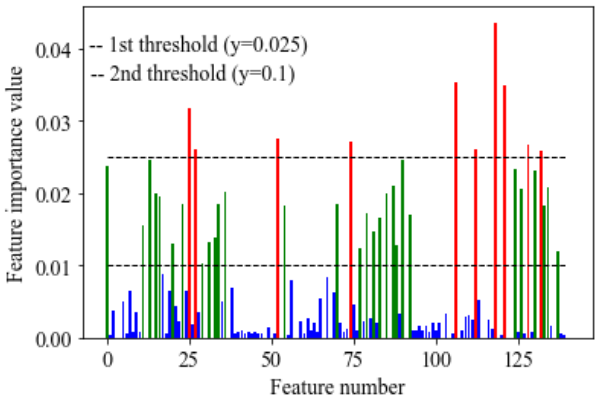

Fig. 6. Feature importance for the sensor placed in the pocket

Foot-mounted sensor The results of the classification for the foot-mounted sensor are given in Table 2. The mean overall accuracy, computed for 3 random folds, is 99.76% and the mean Macro-averaged F1-Score is 98.97%. The mean F1-Score relative to kick-scooter is 99.00%.

Waist-attached sensor The results of the classification for the waist-attached sensor are given in Table 3. The mean overall accuracy is 99.72% and the mean Macro-averaged F1-Score is 98.98%. The mean F1-Score relative to kick-scooter is 99.60%.

Table 2. Confusion Matrix for the foot-mounted sensor using RF algorithm

	Still	Walk	Bike	PT	KS
Still	4339.7	0	5.7	55.7	0.7
Walk	0	6410.7	6.3	40	7.7
Bike	0	0.7	4225.7	17	18.3
PT	112.3	14	48.3	149351	22.3
KS	0	12.7	30	14.3	5445

Table 3. Confusion Matrix for the wais-attached sensor using RF algorithm

	Still	Walk	Bike	PT	KS
Still	4616	1.7	3.7	48	0
Walk	0	8575	18.3	28.3	10
Bike	0	8.3	3981.7	37	0.7
PT	172.7	25.7	60	135040.7	18.7
KS	0.3	2.3	3.3	6	5199.7

Pocket-placed sensor The results of the classification for the sensor located in the pocket are given in Table 4. The mean overall accuracy is 99.81% and the mean Macro-averaged F1-Score is 99,33%. The mean F1-Score relative to kick-scooter is 99.58%.

Table 4. Confusion Matrix for the sensor in the pocket using RF algorithm

	Still	Walk	Bike	PT	KS
Still	4726	0	0	17	0
Walk	0	6831.7	35.5	18.7	17
Bike	2.3	16	6727.3	27.3	0.3
PT	83.3	8	35.7	137562.3	7.7
KS	8.3	10.3	12.7	8.7	7771

5.2 CNN Algorithm

Foot-mounted sensor The results of the classification for the foot-mounted sensor are given in Table 5. The overall accuracy is 97,67% and the Macro-averaged F1-Score is 88,33%. For the kick-scooter, the F1-Score is 94,2%.

Table 5. Matrix for the foot-mounted sensor using the CNN

	Still	Walk	Bike	PT	KS
Still	2103	45	6	532.3	4.7
Walk	32	6106.3	7.7	68.3	46
Bike	2	2.7	4016	137	192.7
PT	2246.3	101.7	145.3	148789	112.3
KS	1.7	24.3	185	77.3	5193.3

Waist-attached sensor The results of the classification for the waist-attached sensor are given in Table 6. The mean overall accuracy is 97.07% and the mean Macro-averaged F1-Score is 87.61%. The kick-scooter relative mean F1-Score is 91.8%.

Table 6. Confusion Matrix for the waist-attached sensor using the CNN

	Still	Walk	Bike	PT	KS
Still	2614.7	21	6.7	718.7	1
Walk	176.7	8439	38	118.7	41.7
Bike	12	12.3	3670.3	176	114.3
PT	2030.7	151.3	284.3	133797.7	90
KS	12	50.3	368.7	216	5003

Sensor placed in the trouser's pocket The results of the classification for the sensor put in the pocket are given in Table 7. The mean overall accuracy is 94.34% and the mean Macro-averaged F1-Score is 90.77%. The mean F1-Score relative to the kick-scooter is 94.15%.

Table 7. Confusion Matrix for the sensor in the pocket using the CNN

	Still	Walk	Bike	PT	KS
Still	3082.7	56.3	10	641	4
Walk	9	6546.7	18.7	33.7	54
Bike	29.3	19.7	6150	133	167
PT	1804	62.7	122.3	136707.7	133
KS	14	41.7	345	180.7	7562

5.3 Discussion of the results

Fig. 7 recapitulates the F1-Scores obtained for the class kick-scooter using RF and CNN. It is observed that RF outperforms the CNN. One possible explanation for this result is that RF is itself an embedded feature-selection method, which is not the case for the CNN. More globally, model selection in this work suggests that RF achieves a high classification performance while not requiring an important tuning effort as compared with the CNN.

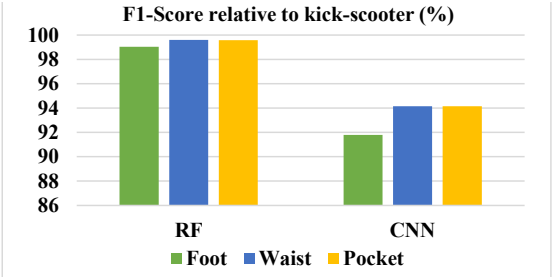

Fig. 7. F1-Score relative to kick-scooter with CNN and RF algorithms for the 3 sensor placements

A frequent error was the confusion of KS, biking, and PT. In fact, pushing and biking may result in similar signal patterns. For PT, these confusions seem to be more related to cruising phases either for bike or KS. In fact, the signals are flat if the user is neither pushing nor biking, which is also the case in PT. For the same reason, confusions between PT and static are also frequent.

6. CONCLUSION

In this work, we have explored the possibility of detecting kick-scooters among other urban transportation modes. The classification included being still, walking, biking, being in public transport and kick-scooter riding. The obtained overall accuracy and F1-Score were above 99% for RF, and above 91% for the CNN algorithm, which is rather promising. In future work, a refining of kick-scooter modalities should be considered to separate pushing from cruising patterns.

REFERENCES

Ahmed, M., Antar, A.D., Hossain, T., Inoue, S., and Ahad, M.A.R. (2019). Poiden: position and orientation independent deep ensemble network for the classification of locomotion and transportation modes. In

UbiComp/ISWC '19 Adjunct, 674–679. London, United Kingdom.

Asci, G. and Guvensan, M.A. (2019). A novel input set for lstm-based transport mode detection. In *International Conference on Pervasive Computing and Communications Workshops (PerCom Workshops)*, 107–112. Kyoto, Japan.

Ballı, S. and Sağbaş, E.A. (2017). Diagnosis of transportation modes on mobile phone using logistic regression classification. *IET Software*, 12(2), 142–151.

Carpineti, C., Lomonaco, V., Bedogni, L., Di Felice, M., and Bononi, L. (2018). Custom dual transportation mode detection by smartphone devices exploiting sensor diversity. In *International Conference on Pervasive Computing and Communications Workshops (PerCom Workshops)*, 367–372. Athens, Greece.

Coroamă, V.C., Türk, C., and Mattern, F. (2019). Exploring the usefulness of bluetooth and wifi proximity for transportation mode recognition. In *Adjunct Proceedings of the ACM International Joint Conference on Pervasive and Ubiquitous Computing and Proceedings of the ACM International Symposium on Wearable Computers*, 37–40. New York, United States.

Fang, S.H., Fei, Y.X., Xu, Z., and Tsao, Y. (2017). Learning transportation modes from smartphone sensors based on deep neural network. *IEEE Sensors*, 17(18), 6111–6118.

Gong, H., Chen, C., Bialostozky, E., and Lawson, C.T. (2012). A gps/gis method for travel mode detection in new york city. *Computers, Environment and Urban Systems*, 36(2), 131–139.

Gonzalez, P.A., Weinstein, J.S., Barbeau, S.J., Labrador, M.A., Winters, P.L., Georggi, N.L., and Perez, R. (2010). Automating mode detection for travel behaviour analysis by using global positioning systems-enabled mobile phones and neural networks. *IET Intelligent Transport Systems*, 4(1), 37–49.

Hossin, M. and Sulaiman, M. (2015). A review on evaluation metrics for data classification evaluations. *International Journal of Data Mining & Knowledge Management Process*, 5(2), 1.

Huang, H., Cheng, Y., and Weibel, R. (2019). Transport mode detection based on mobile phone network data: A systematic review. *Transportation Research Part C: Emerging Technologies*, 101, 297–312.

Kostrzewska, M. and Macikowski, B. (2017). Towards hybrid urban mobility: Kick scooter as a means of individual transport in the city. *IOP Conference Series: Materials Science and Engineering*, 245, 1–10.

Liang, X. and Wang, G. (2017). A convolutional neural network for transportation mode detection based on smartphone platform. In *international conference on mobile Ad Hoc and sensor systems (MASS)*, 338–342. Orlando, FL, USA.

Liang, X., Zhang, Y., Wang, G., and Xu, S. (2019). A deep learning model for transportation mode detection based on smartphone sensing data. *IEEE Transactions on Intelligent Transportation Systems*, 21(12), 5223–5235.

Lorintiu, O. and Vassilev, A. (2016). Transportation mode recognition based on smartphone embedded sensors for carbon footprint estimation. In *International Conference on Intelligent Transportation Systems (ITSC)*, 1976–1981. Rio de Janeiro, Brazil.

McKenzie, G. (2020). Urban mobility in the sharing economy: A spatio-temporal comparison of shared mobility services. *Computers, Environment and Urban Systems*, 79, 1–10.

Prentow, T.S., Blunck, H., Kjærgaard, M.B., and Stisen, A. (2015). Towards indoor transportation mode detection using mobile sensing. In *International Conference on Mobile Computing, Applications, and Services*, 259–279. Berlin, Germany.

Semanjski, I., Gautama, S., Ahas, R., and Witlox, F. (2017). Spatial context mining approach for transport mode recognition from mobile sensed big data. *Computers, Environment and Urban Systems*, 66, 38–52.

Shafique, M.A. and Hato, E. (2015). Use of acceleration data for transportation mode prediction. *Transportation*, 42(1), 163–188.

Shiv, A. et al. (2018). *Analysis of last mile transport pilot: Implementation of the model and its adaptation among local citizens*. Master's thesis, AALTO University, Espoo, Finland.

Su, X., Yao, Y., He, Q., Lu, J., and Tong, H. (2017). Personalized travel mode detection with smartphone sensors. In *International Conference on Big Data (Big Data)*, 1341–1348. IEEE.

Taia Alaoui, F., Fourati, H., Kibangou, A., Robu, B., and Vuillerme, N. (2021). Urban transportation mode detection from inertial and barometric data in pedestrian mobility. *IEEE Sensors*, 1–9. doi:10.1109/JSEN.2021.3065848.

Wang, L., Gjoreski, H., Ciliberto, M., Mekki, S., Valentin, S., and Roggen, D. (2019). Enabling reproducible research in sensor-based transportation mode recognition with the sussex-huawei dataset. *IEEE Access*, 7, 10870–10891.

Wang, L., Gjoreskia, H., Murao, K., Okita, T., and Roggen, D. (2018). Summary of the sussex-huawei locomotion-transportation recognition challenge. In *ACM international joint conference and international symposium on pervasive and ubiquitous computing and wearable computers*, 1521–1530. Singapore.

Xiao, G., Juan, Z., and Zhang, C. (2015). Travel mode detection based on gps track data and bayesian networks. *Computers, Environment and Urban Systems*, 54, 14–22.

Yanyun, G., Fang, Z., Shaomeng, C., and Haiyong, L. (2017). A convolutional neural networks based transportation mode identification algorithm. In *International Conference on Indoor Positioning and Indoor Navigation (IPIN)*, 1–7. Sapporo, Japan.

Yu, M.C., Yu, T., Wang, S.C., Lin, C.J., and Chang, E.Y. (2014). Big data small footprint: The design of a low-power classifier for detecting transportation modes. *Proceedings of the VLDB Endowment*, 7(13), 1429–1440.

Zhao, H., Hou, C., Alrobassy, H., and Zeng, X. (2019). Recognition of transportation state by smartphone sensors using deep bi-lstm neural network. *Journal of Computer Networks and Communications*, 2019, 1–11.

Zuo, T., Wei, H., Chen, N., and Zhang, C. (2020). First-and-last mile solution via bicycling to improving transit accessibility and advancing transportation equity. *Cities*, 99, 1–14.